Journal of African Earth Sciences 106 (2015) 99–107

Contents lists available at ScienceDirect

Journal of African Earth Sciences

journal homepage: www.elsevier.com/locate/jafrearsci

Rare earth elements, S and Sr isotopes and origin of barite from Bahariya Oasis, Egypt: Implication for the origin of host iron ores

Hassan M. Baioumy *

School of Physics, Universiti Sains Malaysia, 11800 USM, Penang, Malaysia

ARTICLE INFO

Article history:
Received 12 November 2014
Received in revised form 20 March 2015
Accepted 21 March 2015
Available online 28 March 2015

Keywords:
Barite
Iron ores
Egypt
Sulfur isotopes
Strontium isotopes
REE contents

ABSTRACT

Based on their occurrences and relation to the host iron ores, barites are classified into: (1) fragmented barite occurs as pebble to sand-size white to yellowish white barite along the unconformity between the Bahariya Formation and iron ores, (2) interstitial barite is present as pockets and lenses of large and pure crystals inside the iron ores interstitial barite inside the iron ores, and (3) disseminated barite occurs at the top of the iron ores of relatively large crystals of barite embedded in hematite and goethite matrix. In the current study, these barites have been analyzed for their rare earth elements (REE) as well as strontium and sulfur isotopes to assess their source and origin as well as the origin of host iron ores.

Barite samples from the three types are characterized by low ΣREE contents ranging between 12 and 21 ppm. Disseminated barite shows relatively lower ΣREE contents (12 ppm) compared to the fragmented (19 ppm) and interstitial (21 ppm) barites. This is probably due to the relatively higher Fe_2O_3 in the disseminated barite that might dilute its ΣREE content. Chondrite-normalized REE patterns for the three barite mineralizations exhibit enrichment of light rare earth elements (LREE) relative to heavy rare earth elements (HREE) as shown by the high $(La/Yb)_N$ ratios that range between 14 and 45 as well as pronounced negative Ce anomalies varying between 0.03 and 0.18. The $^{87}Sr/^{86}Sr$ ratios in the analyzed samples vary between 0.707422 and 0.712237. These $^{87}Sr/^{86}Sr$ values are higher than the $^{87}Sr/^{86}Sr$ ratios of the seawater at the time of barite formation (Middle Eocene with $^{87}Sr/^{86}Sr$ ratios of 0.70773 to 0.70778) suggesting a contribution of hydrothermal fluid of high Sr isotope ratios. The $\delta^{34}S$ values in the analyzed barites range between 14.39‰ and 18.92‰. The lower $\delta^{34}S$ ratios in the studied barites compared with those of the seawater at the time of barite formation (Middle Eocene with $\delta^{34}S$ ratios of 20–22‰) is attributed to a possible contribution of hydrothermal fluid of low $\delta^{34}S$ values that lowered the $\delta^{34}S$ values in the studied barites.

Rare earth elements distribution and patterns, as well as strontium and sulfur isotopes suggest a mixing of seawater and a hydrothermal fluid as possible sources for barite mineralizations in the Bahariya Oasis. The seawater source is suggested from the low Ce/La ratios, "V" shape of the rare earth patterns and pronounced negative Ce anomalies. On the other hand, the hydrothermal fluid contribution is evident from the low concentrations of rare earth and the deviation in both S and Sr isotopic compositions from those of the seawater during the time of barites formation (Middle Eocene). The relatively heterogeneous Sr and S isotope ratios among the studied barites suggest the Bahariya Formation and Basement Complex as possible sources of the hydrothermal fluids. The similarity in the REE as well as S and Sr isotopic compositions of the three types of barite suggest that they form simultaneously.

As the geology and occurrence of the barites suggest a genetic relationship between these barites and the host iron ores, the mixed seawater and hydrothermal sources model of the barites is still applicable for the source of the host iron ores.

1. Introduction

Barite is widespread in hydrothermal deposits of diverse geological settings and fluid sources, including magmatic (Williams-Jones et al., 2000), metamorphic (Hanor, 2000), or sedimentary basinal hydrothermal fluids (Kontak et al., 2006), as well as ancient and modern oceanic water (Monnin and Cividini, 2006). Barite-bearing deposits form in a variety of ways: fluid-cooling (Pfaff et al., 2010), mixing of two or more fluids (Valenza et al., 2000), intense fluid–rock interaction (Marchev et al., 2002), or bacterial processes (Pfaff et al., 2010).

* Tel.: +60 465335315; fax: +60 46579150.
E-mail address: hassanbaioumy@hotmail.com

http://dx.doi.org/10.1016/j.jafrearsci.2015.03.016
1464-343X/

Strontium and sulfur isotopes have been widely used to examine the source and origin of barite and differentiate between barites of different origins (e.g., Valenza et al., 2000; Marchev et al., 2002; Scotney et al., 2005; Wagner et al., 2005; Marchev and Moritz, 2006; Schwinn et al., 2006). Using the two isotopes systems (Sr and S isotopes) should help to distinguish between different fluid sources, and obtain information about changes in the fluid composition, transport and precipitation mechanisms. Fluid inclusions analysis (e.g., Luders et al., 2001; Gültekin et al., 2003; Bozkaya, 2009) and rare earth elements geochemistry (e.g., Guichard et al., 1979) were also used to examine the source and origin of barite but in less extensive compared to the strontium and sulfur isotopes.

Several deposits of iron ores are located in Bahariya Oasis, Egypt, in El Harra, El Heiz, Ghorabi, El Gedida, and Nasser areas. Nakhla and Shehata (1967) classified these iron ores into four types; (i) pisolitic ores, (ii) hard goethitic ores, (iii) soft ores with relatively high Mn contents, and (iv) ochreous ore. Due to their geological and economic importance, the genesis of these ores has been a matter of scientific discussions for a long time. The origin of these ores is controversial and includes epigenetic-supergene (e.g. El Shazly, 1962; Dabous, 2002), to epigenetic-hypogene (e.g. Nakhla, 1961; Basta and Amer, 1969), volcanogenic (e.g. Tosson and Saad, 1974), hydrothermal-metasomatic (e.g. El Sharkawi et al. (1984), karstification of the pre-existing limestone (e.g., El Aref and Lotfy, 1985), hydrogeneous (e.g., Baioumy et al., 2013), and mixed hydrogeneous and hydrothermal (e.g., Baioumy et al., 2014) origins.

Origin of barite in these iron ores is also the debatable due to its occurrence in some ores (e.g., El Gedida ores) and absence from other ores as well as a source of high barium and sulfur required to precipitate barite in these ores. In addition, no systematic investigations have been performed to examine the origin of these barite mineralizations and their genetic relationship with the host iron ores. Therefore, this work was designed to utilize the geology, rare earth elements geochemistry and S and Sr isotopic signatures of the barite mineralizations from the iron ores of the Bahariya Oasis to examine their source and origin. The origin and source of these barite mineralizations were also used to discuss the possible origin of the host iron ores.

2. Geology and stratigraphy of the barite-bearing iron ores

The Bahariya Oasis is a large depression in the Western Desert of Egypt located about 270 km SW of Cairo (Fig. 1A). Within the depression, the Lower Cenomanian fluviomarine sandstone of the Sabaya Formation (Morsy, 1987) is covered by the sandstone, shales and glauconite of the Lower Cenomanian Bahariya Formation (Soliman and El Badry, 1980). The Bahariya Formation is unconformably overlain by the Upper Cenomanian fluviomarine shale, dolomitic limestone and calcareous sandstone of El the Heiz Formation as well as by the Campanian cherty dolostone, cross-bedded sandstone and phosphatic limestone of the El Haufhuf Formation (Morsy, 1987). The succeeding chalk of the Maastrichtian Khoman Formation overlies conformably El Haufhuf Formation and extends southward with increasing thickness. The Eocene rocks are represented by the limestone of the Lower Eocene Qalamoun Formation (El Shazly, 1962), and the gray and pink crystalline limestone of the Middle Eocene Naqb Qazzun Formation (El Bassyony, 2005). The sandstone, quartzites, shale and silt of the Oligocene Qatrani Formation cover the Bahariya Formation at the top of the conical hills (Morsy, 1987). North of Gebel El Haufhuf, the Oligo-Miocene basaltic and doleritic extrusions are recorded (Meneisy and El Kaleubi, 1975).

Economic sedimentary iron ores with an average of 47.6 wt.% Fe (Said, 1990) occur in the northern part of the Bahariya depression

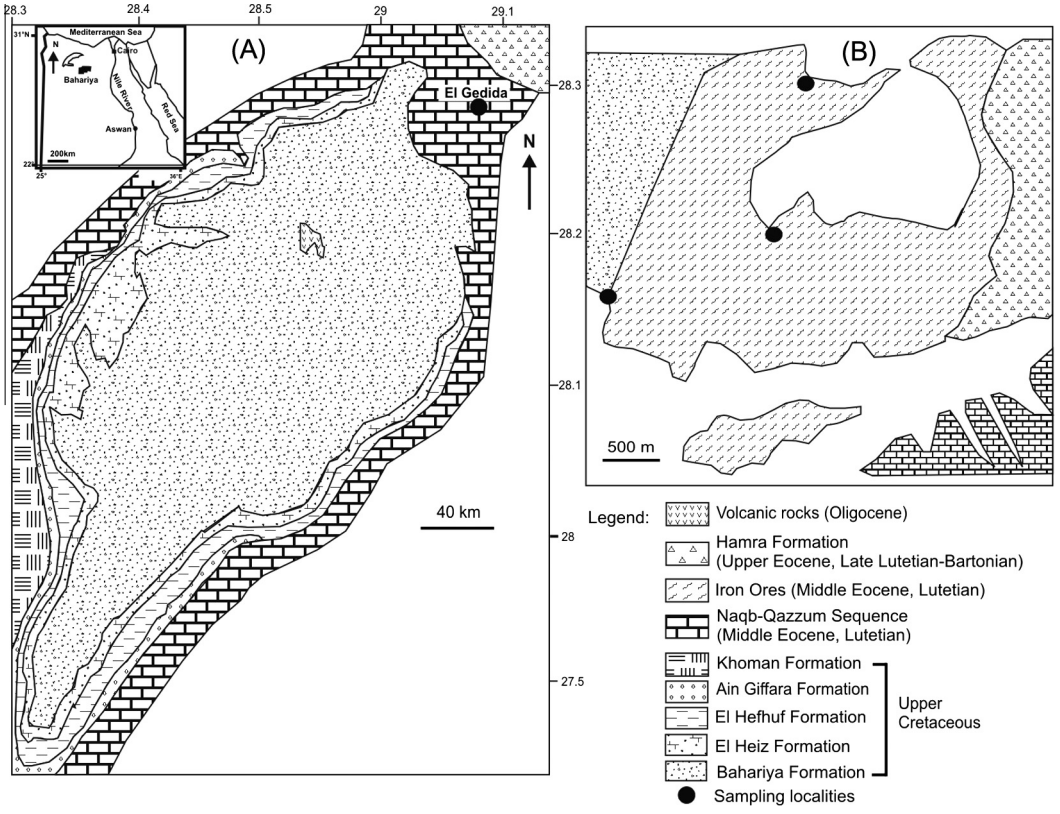

Fig. 1. (A) Generalized geological map of the Bahariya Oasis, Western Desert, Egypt with the location of the studied iron ores (from Catuneanu et al., 2006). (B) Detailed geological map of El Gedida iron ores mine (from El Aref et al., 1999).

in the lower part of the Middle Eocene limestone of the Naqb Qazzun Formation covering an area of 11.7 km^2 with a thickness varying from 2 to 35 m, 9 m on averaging (Said, 1990). The iron ores occur in three areas including the Ghorabi (3.5 km^2), El Harra (2.9 km^2) and El Gedida (15 km^2) areas. According to Baioumy et al. (2013), the iron ores of the Bahariya Oasis are composed mainly of hematite and goethite with some detrital quartz. Mn-bearing minerals in the Mn-rich iron ores occur either as pyrolusite or fine-grained cement-like materials that are dominated by a mixture of manganese oxides and hydroxide minerals such as bixbyite, cryptomelane, aurorite, romanechite, manjiroite, and pyrochroite. Barite mineralizations, the target of this study, occur mainly in the iron ores of El Gedida mine.

The El Gedida iron mine area is an oval shaped depression up to 15 km^2 in area, situated within the degraded cone hills of the Naqb Qazzun Formation (Fig. 1B). The central part of the depression comprises the Cenomanian sandstone and sandy clays of the Bahariya Formation at the base and is overstepped by the Middle

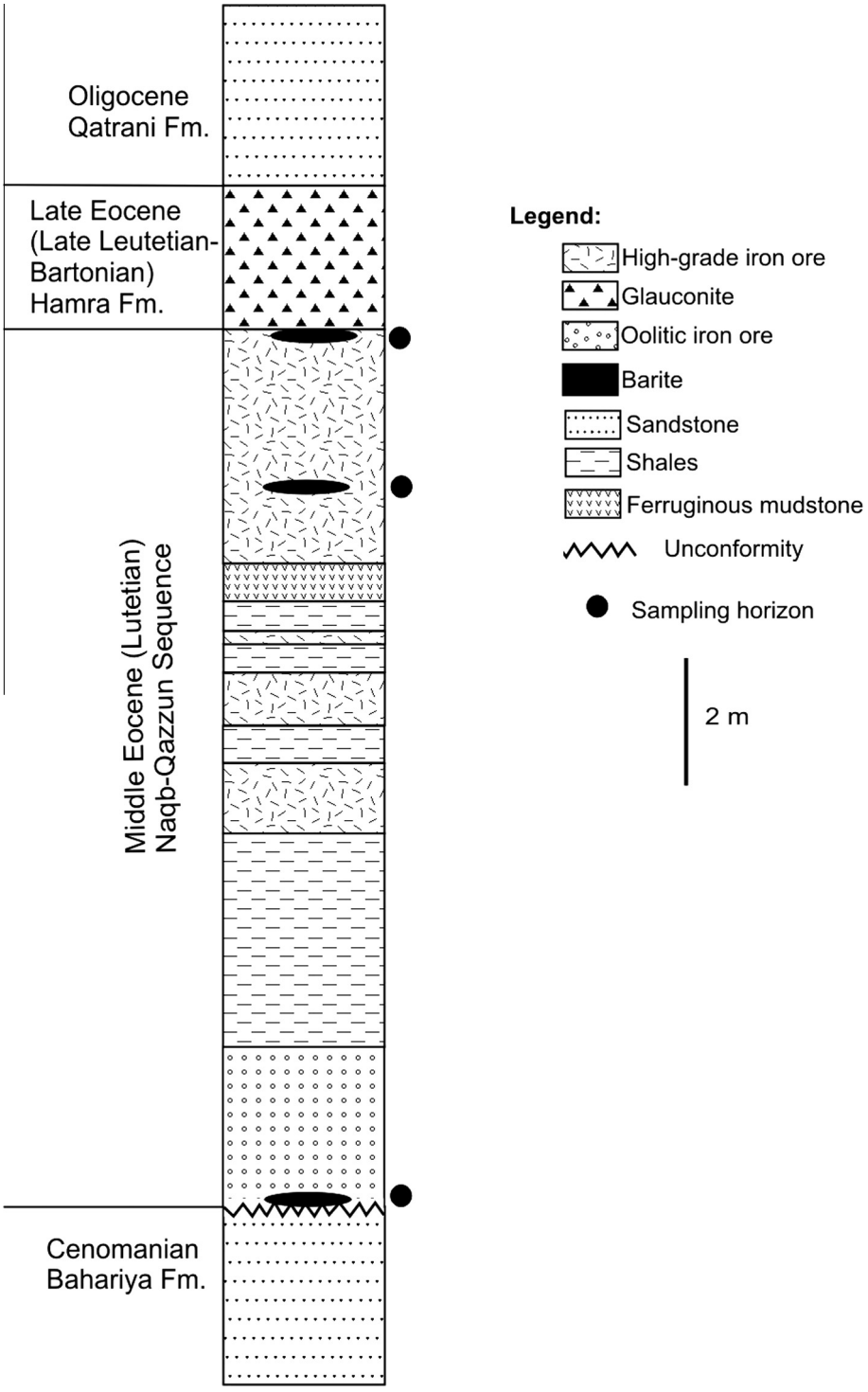

Fig. 2. Stratigraphic columnar section of the iron ores in the Eastern Wadi of El Gedida mine area (A) (From El Aref et al., 1999) with position of the barite mineralizations and samples locations.

Eocene (Lutetian) iron ores of Naqb Qazzun Sequence. In the Eastern and Western Wadi areas of the depression, the iron ore successions are truncated unconformably by Late Eocene (Late Lutetian-Bartonian) glauconites with lateritic ironstone interbeds of the Hamra Formation (e.g., El Aref et al., 1999). The iron ores attain their maximum thickness in the Western and Eastern Wadi areas (up to 35 m), and it is strongly reduced to 11 m in the high central area. The iron ores consist of a pisolitic–oolitic ironstone unit followed by bedded iron ores intercalated with ferruginous mudstones (e.g., El Aref et al., 1999). The thickness of the overlying glauconitic sandstone of the Hamra Formation varies from 25 m in the Western and Eastern Wadis areas to 1 m in the high central area (Fig. 2).

3. Methodology

Nine samples have been collected from the fragmented, interstitial and disseminated barite mineralizations at El Gedida iron ores mine. Representative samples of these barites were subjected to detailed petrographic, mineralogical, and geochemical analyses. Polished and thin sections were prepared from the three barite types and investigated under the optical microscope. A Philips PW 1730 X-ray generator with Fe-filtered Co Kα, run at 40 kV and 30 mA, was used to analyze barite samples. Petrographic and mineralogical analyses were conducted at the Central Metallurgical R & D Institute (CMRDI), Cairo, Egypt.

Fused discs prepared from the three types of barite have been analyzed for major oxides (SiO_2, TiO_2, Al_2O_3, Fe_2O_3, MgO, MnO, CaO, K_2O, Na_2O, and P_2O_5) by XRF using Philips PW 2400 X-ray spectrometer at Tohoku University, Japan. Tube voltage and current for W target was 40 kV and 60 mA, respectively. Loss of ignition (L.O.I.) was obtained by heating sample powders to 1000 °C for 6 h.

Rare earth elements (REE) concentrations of the same samples were determined by an SCIEX-ELAN DRC II ICP-MS at Tohoku University, Japan. The samples powders were digested using alkaline fusion ($NaOH–Na_2O_2$) (e.g. Bayon et al., 2009). About 100 mg of sample powder were weighed carefully, then placed in the crucible with 1.2 g Na_2O_2, 0.6 g NaOH and fused in a muffle furnace at 650 °C for 15 min. After cooling the crucible (~3 min), the melt was dissolved by adding 10 ml of ultra-pure water, then transferred into a PTFE beaker. The crucible was rinsed with an additional 20 ml of ultra-pure water. The PTFE beaker heated at 130 °C on a hotplate for two hours. The solution was then rinsed into a pre-cleaned centrifuge tube and centrifuged for 3 min at 3000 rpm. The clear supernatant was decanted and the centrifuge tube was filled with 15 ml of ultra-pure water, stirred, and then centrifuged again. The samples were then dissolved in 6M HCl, transferred into acid-cleaned HDPE bottles, and stored as 'mother' solution (~20 ml). Finally, a few hours before measurement, an aliquot of the 'mother' solution was dried down, taken up in 200 µl concentrated HNO_3 acid, and diluted with 10 ml ultra-pure water.

For sulfur isotopes measurements, the barites samples were rinsed with warm di-ionized water to remove the halogens in salts, and samples were dried and measured directly on the instrument. The samples were combusted in an elemental analyzer to form SO_2 gas which was introduced into the mass spectrometer. Analyses were standardized using NIST 127 in the Stable Isotope Research Facility (SIRF), Indiana University, USA and two internal laboratory standards to bracket the range of isotopic values observed in the samples. Sulfur isotope values are reported relative to the Vienna Canyon Diablo Troilite (VCDT) and in terms of a $\delta^{34}S_{VCDT}‰$ (e.g. Jiang et al., 2008). The samples were analyzed in duplicate where sample abundance permitted and the replicates were ±0.3 per mil or less.

To dissolve barite for the determination of Sr isotopes, the procedure (i.e. aqueous sodium carbonate digestion technique) proposed by Breit et al. (1985) was followed. 10 mg of purified barite, 100 mg of sodium carbonate (Suprapur®, Kanto Chemical), and 2 ml of Milli Q water were placed in a 7 ml Teflon PFA screw cap vial (Savilex Corp., Minnetonka, Minnesota). The tightly closed vial was kept on a hot plate for 12 h at 90 °C; then, the solid residue was washed thoroughly with Milli Q water to remove sodium and sulfate. The residue was then dissolved with 1 ml of 2 M HNO_3. Strontium separation was carried out using a shrink fit Teflon column filled with 0.3 ml of Sr spec resin (50–100 µm particle size; Eichrom Technologies, Inc., Darien, Illinois). The column was washed with 1 ml of Milli Q water and conditioned with 0.5 ml of 2 M HNO_3. 0.5 ml of sample solution (2 M HNO_3) was loaded on the column that was washed with 1.2 ml of 8 M HNO_3 to remove Ba. The column was then treated with 0.4 ml of 2 M HNO_3. Sr was stripped with 1 ml of 0.01 M HNO_3, and the Sr fraction was evaporated to dryness. The residue was dissolved with 10 µl of 1M H_3PO_4, 1 µl of which (corresponding to ~2 µg of Sr) was loaded onto a previously outgassed Ta filament. Sr isotopic compositions were determined using Finnigan MAT262 at the University of the Ryukyus, Japan. The Sr standard NIST 987 gave $^{87}Sr/^{86}Sr = 0.710247 \pm 0.000020$ (2σ; $n = 12$).

4. Results

4.1. Field occurrence and mineralogy of barite

Based on their occurrences and relation to the host iron ores, barites in El Gedida area occurs in three modes. From bottom to top of the iron-bearing sequence, they are the fragmented, interstitial and disseminated barite. Fragmented barite occurs as pebble to sand-size white to yellowish white barite along the unconformity surface between the sandstone of the Bahariya Formation and the iron-bearing horizon of the Naqb Qazzun sequence (Fig. 3A). Geologists at El Gedida iron ores mine call this type as detrital barite. The thickness of this barite horizon ranges between 20 cm and 1 m as horizontal bed-like. Interstitial barite is present as pockets and lenses ranging in diameter from few centimeters to 50 cm inside the iron ores of the Naqb Qazzun sequence (Fig. 3B). Barite of this type occurs as aggregates of white or colorless large crystals (up to 5 cm long) and is exploited for commercial uses by oil companies due to its purity and high specific gravity. The disseminated barite occurs at the top of the iron-bearing horizon of the Naqb Qazzun sequence as beds and lenses 50 cm to 2 m thick of relatively large crystals of barite embedded in hematite and goethite matrix (Fig. 3C). This type of varies in color from reddish to yellowish white based on the contents of iron.

XRD analysis of the three types of barite shows that the interstitial barite is composed entirely of barite. Fragmented barite is composed of barite with traces of quartz, while the disseminated barite is composed of hematite and goethite in addition to barite. Under optical microscope, interstitial and fragmented barite occurs as almost pure barite with some Fe-rich veinlets in the fragmented barite. The disseminated barite occurs as large grey crystals inside the Fe-bearing minerals (hematite and goethite).

4.2. Major oxides and rare earth elements

Distribution of major oxides in the fragmented, interstitial and disseminated barites is summarized in Table 1. Except from the $BaSO_4$ contents that range between 75 and 97.5 (wt.%), barite samples exhibit low concentrations of major oxides such as SiO_2 (0.17–1.49 wt.%), Al_2O_3 (0.3–0.9 wt.%), TiO_2 (0.13–0.44 wt.%), MgO (0.07–0.15 wt.%), K_2O (0.14–0.25 wt.%), Na_2O (0.54–0.71 wt.%), P_2O_5

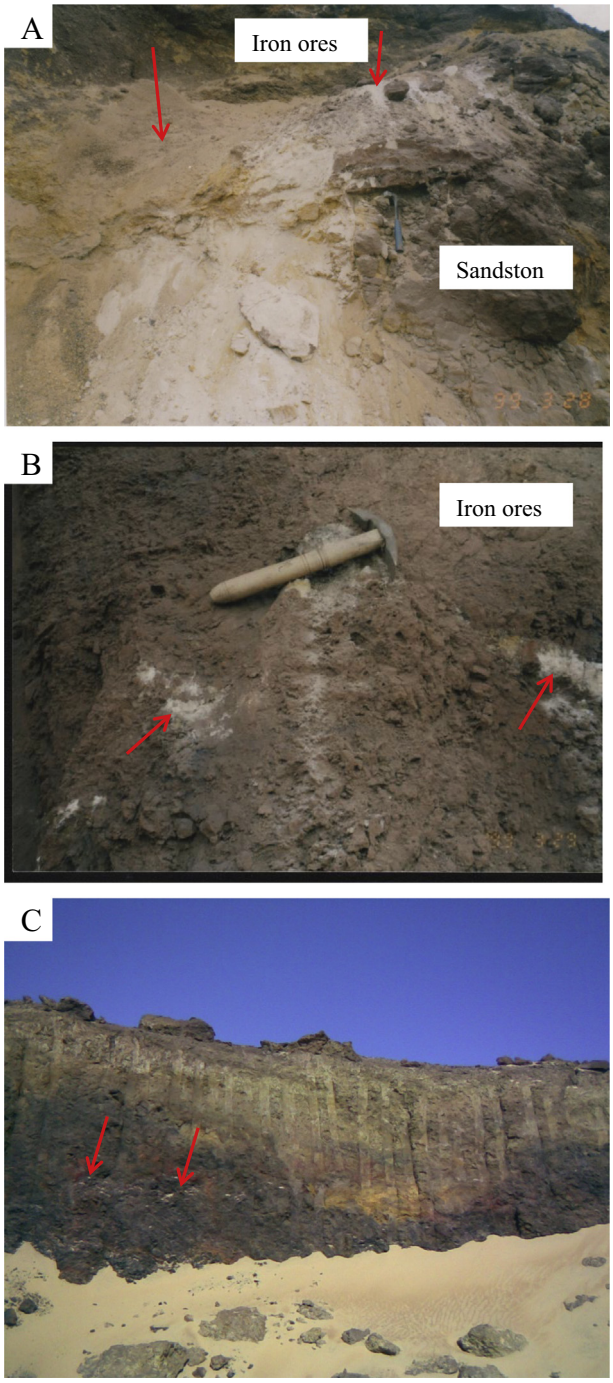

Fig. 3. Field photos show the modes of occurrences of barite in the iron ores at Bahariya Oasis. (A) Fragmented barite along the unconformity between the Bahariya Formation and Naqb Qazzun iron-bearing sequence (red arrows). (B) White barite as small lenses and interstitial (red arrows) inside the iron ore (Hammer length is about 25 cm). (C) Disseminated barite at the top of the iron ores horizon at El Gedida mine (arrows). (For interpretation of the references to color in this figure legend, the reader is referred to the web version of this article.)

(0.05–0.18 wt.%). CaO and MnO occur in very low concentrations lower than 0.1 wt.%. The disseminated barite shows relatively high Fe_2O_3 content (23.29 wt.%) compared to the interstitial and fragmented barite samples (0.19 wt.%). On the other hand, fragmented barite has slightly higher SiO_2 and Al_2O_3 compared to interstitial and disseminated barite samples probably due to the occurrence of silicates inclusions from the underlying sandstone of the Bahariya Formation.

Table 1
Major oxides distributions (wt.%) in the three types of barite mineralizations from the Bahariaya Oasis measured by XRF.

Major oxides	Fragmented barite	Interstitial barite	Disseminated barite
$BaSO_4$	95.99	97.45	75.02
Fe_2O_3	0.19	0.19	23.29
SiO_2	1.49	0.49	0.17
Na_2O	0.71	0.54	0.61
MgO	0.15	0.10	0.07
Al_2O_3	0.90	0.30	0.38
P_2O_5	0.14	0.05	0.18
K_2O	0.25	0.15	0.14
CaO	0.01	0.01	0.01
TiO_2	0.13	0.37	0.44
MnO	0.08	0.08	0.08
Sum	100.04	99.73	100.39

Table 2
Rare earth elements contents (ppm) in the three types of barite mineralizations from the Bahariaya Oasis measured by ICP-MS.

Rare earth elements	Fragmented barite	Interstitial barite	Disseminated barite
La	10.23	11.37	4.15
Ce	0.51	0.56	1.34
Pr	0.08	0.09	0.20
Nd	0.28	0.31	0.80
Sm	1.41	1.57	0.61
Eu	3.48	3.87	3.35
Gd	2.32	2.58	1.05
Tb	0.00	0.00	0.05
Dy	0.03	0.04	0.32
Ho	0.01	0.01	0.07
Er	0.03	0.04	0.17
Tm	0.01	0.01	0.02
Yb	0.15	0.17	0.20
Lu	0.29	0.32	0.11
ΣREE	18.83	20.94	12.44
Ce/La	0.05	0.05	0.32
$(La/Yb)_N$	44.99	44.99	14.27
Eu/Eu*	5.88	5.88	12.81
Ce/Ce*	0.03	0.03	0.18

Rare earth elements (REE) concentrations in the fragmented, interstitial and disseminated barites are summarized in Table 2. It shows that the ΣREE contents in the barite samples are very low ranging between 12 and 21 ppm. There is no significant difference in the REE concentrations among the fragmented (ΣREE = 19 ppm) and interstitial (ΣREE = 21 ppm) barites. Disseminated barite shows lower ΣREE contents (ΣREE = 12 ppm) compared to the fragmented and interstitial barites probably due to the higher Fe_2O_3 content in the disseminated barite that might have diluted the REE contents in this barite. The REE patterns were normalized to the chondrite REE concentrations, which are average and reference values (e.g. Boynton, 1984; McLennan, 1989). The Eu anomaly is calculated as $E/E^* = (Eu/Eu_N)/[(Sm/Sm_N)^{0.5} \times (Gd/Gd_N)^{0.5}]$, the Ce anomaly is calculated as $Ce/Ce^* = (Ce/Ce_N)/[(La/La_N)^{0.5} \times (Pr/Pr_N)^{0.5}]$ and LREE enrichment relative to HREE as $(La/Yb)_N = (La/La_N)/(Yb/Yb_N)$ following Braun et al. (1998). Chondrite-normalized REE patterns for the three barite types (Fig. 4) exhibit LREE enrichment relative to HREE as shown by $(La/Yb)_N$ ratios range between 14 and 45. They also show pronounced negative Ce anomalies ranging between 0.03 and 0.18.

4.3. Strontium isotopes

The $^{87}Sr/^{86}Sr$ ratios of samples represent the fragmented, interstitial and disseminated barites are shown in Table 3. Although the

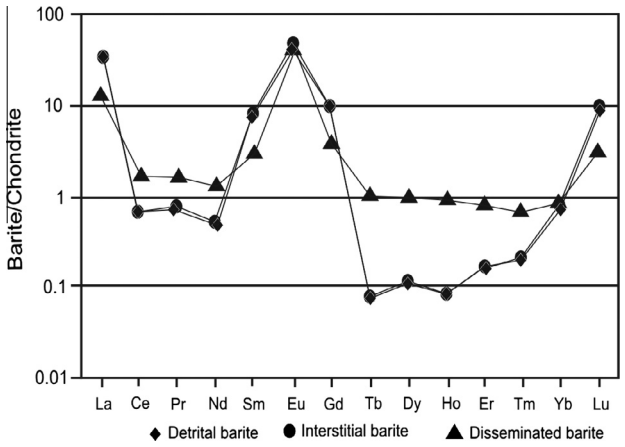

Fig. 4. Chondrite-normalized REE patterns for the fragmented, interstitial and disseminated barites from the Bahariya iron ores.

Table 3
Strontium isotopic compositions (‰) for the three types of barite mineralizations from the Bahariaya Oasis.

Barite mineralization	Sample	Sr isotopic composition (‰)	Sr isotopic composition (‰) of Middle Eocene seawater (e.g. Veizer, 1989)
Fragmented	1–2	0.710808	0.70773–0.70778
	1–3	0.711067	
	2–1	0.709688	
	2–2	0.709715	
	2–3	0.709760	
	Average	0.710208	
Interstitial	5–1	0.708704	
	5–2	0.708936	
	5–3	0.708696	
	6–1	0.712055	
	6–2	0.711464	
	6–3	0.709194	
	Average	0.709842	
Disseminated	3–1	0.707422	
	3–2	0.711120	
	3–3	0.709664	
	4–1	0.709827	
	4–2	0.710543	
	4–3	0.712237	
	Average	0.710136	

$^{87}Sr/^{86}Sr$ ratios in the studied samples are slightly variable, no particular trend in these values among the different types of barite mineralizations. The $^{87}Sr/^{86}Sr$ ratios vary between 0.707422 and 0.712237. The $^{87}Sr/^{86}Sr$ ratios in the fragmented barite range from 0.709688 to 0.711067, while the $^{87}Sr/^{86}Sr$ ratios range from 0.708696 to 0.712055 in the interstitial barite and the ratios vary between 0.707422 and 0.712237 in the disseminated barite.

4.4. Sulfur isotopes

The sulfur isotopic composition $\delta^{34}S$ of samples represent the fragmented, interstitial and disseminated barites are listed in Table 4. Although the $\delta^{34}S$ values in the studied samples are variable, no definite trend in these values among the different types of barite mineralizations. The $\delta^{34}S$ values in the analyzed samples vary between 14.39‰ and 18.92‰. In the fragmented barite the ratios range from 14.39 to 15.62 ‰, while in the interstitial barite the $\delta^{34}S$ values range from 14.94‰ to 18.92‰ and in the disseminated barite the ratios vary between 16.69‰ and 18.19‰.

Table 4
Sulphur isotopic compositions (‰) for the three types of barite mineralizations from the Bahariaya Oasis.

Barite mineralization	Sample	Sulfur isotopes (‰)	S isotopic composition (‰) of Middle Eocene seawater (e.g. Claypol et al., 1980; Paytan et al., 1998; Bottrell and Newton, 2006)
Fragmented	DB 1	15.16	20–22
	DB 2	15.62	
	DB 3	15.31	
	DB 4	14.39	
	DB 5	15.60	
	Average	15.22	
Interstitial	AB 1	15.98	
	AB 2	16.81	
	AB 3	15.55	
	AB 4	16.87	
	AB 6	18.92	
	AB 7	14.94	
	Average	16.51	
Disseminated	IB 1	18.09	
	IB 2	16.69	
	IB 3	18.19	
	IB 4	17.34	
	Average	17.58	

5. Discussion

5.1. Barium source for the barites

Source and origin of the three studied barite types will be discussed here based on their rare earth geochemistry as well as sulfur and strontium isotopes.

According to Guichard et al. (1979), the mineral barite ($BaSO_4$), which occurs in both terrestrial and marine environments, could offer a rewarding system to study the rare earth geochemistry because: (1) The REE pattern for sea water has a characteristic 'V' pattern and negative Ce anomaly (Hogdahl et al., 1968). (2) Marine sediments are distinct from basic rock or hydrothermal patterns (Goldberg et al., 1963; Haskin et al., 1968) and may distinguish the marine versus magmatic modes of barite formation. (3) The enrichment of Eu(II) at the expense of Eu(III) in barite could reveal redox conditions at the loci of formation. (4) The natural fractionation of rare earth elements by low temperature aqueous minerals such as barites might be useful in interpreting crystallization chemistry, rare-earth solution complexing and the utilization of rare earths for interpreting both diagenetic and late stage magmatic events.

Both the concentrations and patterns of rare earth elements have been applied to distinguish between the marine and non-marine barites. Deep-marine barite is characterized by high concentrations of rare earth elements while land and hydrothermal barites exhibit lower total REE concentrations. In general, deep-marine barites contain 10–100 times more REE than those found on the continents (Guichard et al., 1979). Hein et al. (2007) also reported very low concentrations of REE in the rifted continental margin barite from Southern California that formed from low-temperature hydrothermal fluids that circulated along faults. The three types of barites from the iron ores of the Bahariya Oasis have low rare earth elements concentrations suggesting their possible hydrothermal origin. According to Church and Bernat (1971), the Ce/La ratio is very low in deep-marine barite (Ce/La = 0.33) compared to the terrestrial barite (Ce/La = 1.37). The Ce/La ratios in the three barites analyzed in this study (0.05–0.32) are very close to those of the deep-marine barite, which in turn indicates a deep-marine origin of these barites.

As to the rare earth pattern, deep-marine barites present the chondrite-normalized Eu minimum, but not the negative Ce

anomaly, of sea water, while chondrite normalized positive Eu anomalies are displayed by those varieties of reducing sedimentary and metamorphic origin (e.g. Guichard et al., 1979). Hein et al. (2007) used the light REE enrichment in the Chondrite-normalized REE patterns of the rifted continental margin barite from Southern California to indicate a typical marine hydrothermal origin of this barite. Chondrite-normalized REE patterns for the studied barite samples show LREE enrichment relative to HREE with pronounced negative Ce anomalies. This pattern is very similar to the characteristic 'V' shape pattern of deep-marine barite as does fish bone debris and calcareous oozes (Bernat, 1975). Although Guichard et al. (1979) pointed out that Ce appears to display no characteristic anomaly in any barite type, including those found in the deep sea, the studied barites in the Bahariya iron ores exhibit pronounced negative Ce anomalies. This negative anomaly has been used to characterize the marine (versus volcanogenic) origin of authigenic metalliferous precipitates on mid-ocean ridge systems (Bender et al., 1971).

The $^{87}Sr/^{86}Sr$ ratios don't fractionate during crystallization or dissolution of hydrothermal minerals (Matter et al., 1987) and ^{87}Rb, the parent of ^{87}Sr, cannot be incorporated in the crystal lattice of barite at concentrations higher than 100 ppb (Hofmann and Baumann, 1984), and therefore cannot significantly change the Sr composition of barite over time. Therefore, the Sr isotopes in barite can be used safely to reflect the isotopic ratio of the fluid. If the studied barite precipitates from seawater at that time (Middle Eocene), Sr isotopic composition of barite should be the similar to those of seawater at that time ($^{87}Sr/^{86}Sr$ = 0.70773–0.70778, e.g., Veizer, 1989). Sr isotope ratios of the three types of barite (0.7087–0.7122, except for one data of 0.7074) are higher than those of seawater. Substantial deviation of the Sr isotope ratios of barites from seawater were attributed to modification of the strontium from other sources such as older marine sediments, terrigenous material, meteoric water (e.g. Torres et al., 1996; Aquilina et al., 1997; Canet et al., 2014). According to Staude et al. (2011), barites of hydrothermal origin exhibit relatively high Sr isotopes ratios (0.709–0.720). Fluid-mixing scenario has been postulated as a possible source of barite and mixing ratios from the different sources were calculated based on Sr isotopes (e.g. Staude et al., 2011). Therefore, the higher Sr isotopes ratios in the studied barites compared to the Middle Eocene seawater could support the conclusion derived from the rare earth elements that these barites have a mixed source of seawater and hydrothermal fluid.

The sulfur isotopes ratios are more or less homogeneous and have no significant variations in the three studied barites suggesting a homogeneous or single (common) source for these barites. The S isotopes values of the studied barites range between 14‰ and 19‰, which are lower than those of the Middle Eocene seawater (20–22‰, e.g. Claypol et al., 1980; Paytan et al., 1998; Bottrell and Newton, 2006). According to Staude et al. (2011), barites of hydrothermal origin in general show relatively low S isotopes ratios (1.5–20.0‰). Therefore, the low $\delta^{34}S$ of the studied barites compared to the coeval seawater at Middle Eocene might be due to a contribution from hydrothermal fluid that lowered the S isotopes ratios of these barites.

Staude et al. (2011) used a binary plot between Sr and S isotope ratios to distinguish between different barite groups. Barites from the Bahariya Oasis can be distinguished into two groups using this plot (Fig. 5). A group of five analyses have more radiogenic Sr isotopes values compared to others, although they still have similar S isotopes values. The heterogeneous Sr ratios among the studied barites may indicate a multiple source of the hydrothermal fluid. According to Staude et al. (2011), high Sr isotopic compositions reflect basement-derived brine, while the lower radiogenic Sr compositions represent sedimentary cover fluid. The underlying

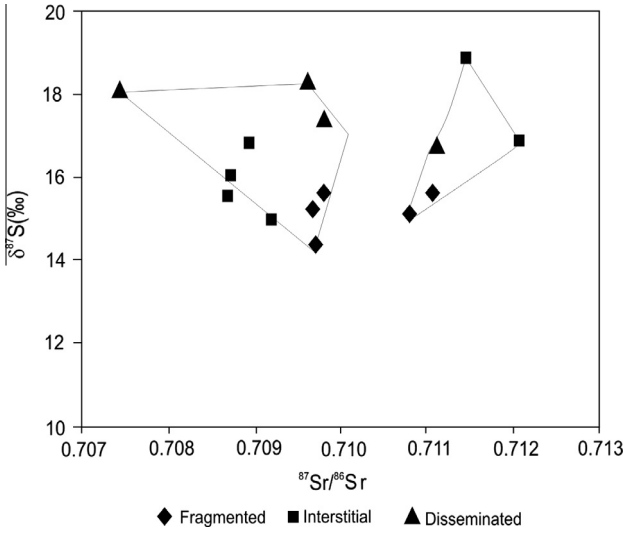

Fig. 5. $\delta^{34}S$ versus $^{87}Sr/^{86}Sr$ binary plot shows that the studied barites can be classified into two groups based on their Sr isotopic compositions.

clastics of the Bahariya Formation as well as the unexposed Basement Complex can be considered the sources of the hydrothermal fluid for the barites in the iron ores of the Bahariya Oasis. Following findings of Staude et al. (2011), clastics of the Bahariya Formation is the possible source of low radiogenic Sr compositions, while the Basement Complex is the possible source of the high Sr isotopic compositions in the studied barites.

5.2. Implication for the origin of the host iron ores

Although the sedimentary iron ores in the Bahariya Oasis have been extensively studied previously with respect to their geology and geochemistry, their origin is still unclear. Barites, the subject of this work, associate these iron ores either underlying or disseminated inside them which indicates a genetic relationship between the barites and host iron ores. Rare earth elements distribution and patterns, as well as strontium and sulfur isotopes, suggested mixed marine and hydrothermal sources of the barite mineralizations. The seawater source of the barites has been indicated from the low Ce/La ratios, "V" shape of the rare earth pattern and pronounced negative Ce anomalies. On the other hand, the hydrothermal source contribution was evident from the low concentrations of rare earth as well as the modification of both S and Sr isotopic compositions of the seawater at the time of barite formation (i.e. Middle Eocene).

Geological observations indicate the close association of barites with the iron ores at their base, inside and at the top of them. This in turn suggests a genetic relationship between these barites and the host iron ores. Therefore, the same mixed seawater and hydrothermal fluid model for the barites can also be applied for the source of the host iron ores. The hydrogeneous origin of these iron ores have been postulated by Baioumy et al. (2013) based on detailed mineralogical, petrographic and geochemical investigations on the high-Mn iron ores in the same area (El Gedida iron mine). Moreover, a mixed source of seawater and hydrothermal fluids were suggested for the iron ores in the Bahariya Oasis by Baioumy et al. (2014) based on trace and rare earth elements geochemistry of these ores.

6. Conclusions

Barite mineralizations that associate the iron ores in the Bahariya Oassis occur in three modes, namely; fragmented barite

underlying the iron ores, interstitial barite inside the iron ores and disseminated or disseminated barite at the top of the iron-bearing succession. Rare earth elements distribution and patterns as well as strontium and sulfur isotopes of these barites suggest mixed source of seawater and hydrothermal fluid for the barite mineralizations. The seawater source has been indicated from the low Ce/La ratios, "V" shape of the rare earth pattern and pronounced negative Ce anomalies. In the meantime, the contribution from the hydrothermal fluid was evident from the low concentrations of rare earth elements and deviation in both S and Sr isotopic compositions from those of the seawater at the time of barites formation (Middle Miocene). The clastics of the Bahariya Formation and Basement Complex can be the source of the hydrothermal fluids. The three types of studied barite probably form simultaneously as indicated from the similarity in their REE as well as S and Sr isotopic compositions. As the geology and occurrence of the barites suggest a genetic relationship between these barites and the host iron ores, the same mixed seawater and hydrothermal fluid model for barites is still applicable for the source of the host iron ores.

Acknowledgments

The author thanks Dr. Ryuichi Shinjo from University of the Ryukyus, Japan for his technical support of this work through analyzing the barite samples for Sr isotopes. Thanks also extend to Dr. Erika R. Elswick for sulfur isotopes analyses in the Analytical Geochemistry Laboratory, Department of Geological Sciences, Indiana University, USA. Author is very much grateful to Dr. Naotatsu Shikazono and Dr. Yasumasa Ogawa from Tohoku University, Japan for REE analyses.

References

Aquilina, L., Dia, A.N., Boulegue, J., Bourgois, J., Fouillac, A.M., 1997. Massive barite deposits in the convergent margin off Peru: implications for fluid circulation within subduction zones. Geochim. Cosmochim. Acta 61, 1233–1245.

Baioumy, H.M., Khedr, M.Z., Ahmed, A.H., 2013. Mineralogy, geochemistry and origin of Mn in the high-Mn iron ores, Bahariya Oasis, Egypt. Ore Geol. Rev. 53, 63–76.

Baioumy, H.M., Ahmed, H.H., Mohamed, Z.K., 2014. A mixed hydrogeneous and hydrothermal origin of the Bahariya iron ores, Egypt: Evidences from the trace and rare earth elements geochemistry. J. Geochem. Explor. 146, 149–162.

Basta, E., Amer, H., 1969. El Gedida iron ores and their origin, Bahariya Oases, Egypt. Econ. Geol. 64, 424–444.

Bayon, G., Barrat, J.A., Etoubleau, J., Benoit, M., Bollinger, C., Révillon, S., 2009. Determination of rare earth elements, Sc, Y, Zr, Ba, Hf and Th in geological samples by ICP-MS after Tm addition and alkaline fusion. Geostand. Geoanal. Res. 33, 51–62.

Bender, M., Broecker, W., Gornitz, V., Miduel, U., Kay, R., Suns, S., 1971. Geochemistry of three cores from the east Pacific rise. Earth Planet. Sci. Lett. 12, 425.

Bernat, M., 1975. Les isotopes de Uranium et du Thorium et les terresrares dans l'environment marin. Cah. Orstom Ser. Geol. 7 (1), 65–83.

Bottrell, S.H., Newton, R.J., 2006. Reconstruction of changes in global sulfur cycling from marine sulfate isotopes. Earth-Sci. Rev. 75, 59.

Boynton, W.V., 1984. Geochemistry of the REE: meteorite studies. In: Henderson (Ed.), Rare Earth Element Geochemistry. Elsevier, pp. 63–114.

Bozkaya, G., 2009. Fluid inclusion and stable isotope (O, H and S) evidence for the origin of the Balcilar vein type barite-galena mineralization in Çanakkale, Biga Peninsula, NW Turkey. J. Geochem. Explor. 101, 8.

Braun, J.J., Viers, J., Dupré, B., Polve, M., Ndam, J., Muller, J.P., 1998. Solid/liquid REE fractionation in the lateritic system of Goyoum, East Cameroon: the implication for the present dynamics of the soil covers of the humid tropical regions. Geochim. Cosmochim. Acta 62, 273–299.

Breit, G.N., Simmons, E.C., Goldhaber, M.B., 1985. Dissolution of barite for the analysis of strontium isotopes and other chemical and isotopic variations using aqueous sodium carbonate. Chem. Geol. 52, 333–336.

Canet, C., Anadón, P., González-Partida, E., Alfonso, P., Rajabi, A., Pérez-Segura, E., Alba-Aldave, L.A., 2014. Paleozoic bedded barite deposits from Sonora (NW Mexico): evidence for a hydrocarbon seep environment of formation. Ore Geol. Rev. 56, 292–300.

Catuneanu, O., Khalifa, M.A., Wanas, H.A., 2006. Sequence stratigraphy of the Lower Cenomanian Bahariya Formation, Bahariya Oasis, Western Desert, Egypt. Sediment. Geol. 190, 121–137.

Church, T.M., Bernat, M., 1971. Thorium and uranium in marine barite. Earth Planet. Sci. Lett. 14, 139.

Claypol, G.E., Holster, W.T., Kaplan, I.R., Sakai, H., Zak, I., 1980. The age curves of sulphur and oxygen in marine sulphate and their mutual interpretations. Chem. Geol. 28, 199–260.

Dabous, A.A., 2002. Uranium isotopic evidence for the origin of the Bahariya iron deposits, Egypt. Ore Geol. Rev. 19, 165–186.

El Aref, M.M., Lotfy, Z.H., 1985. Genetic karst significance of the iron ore deposits of El Bahariya Oasis, Western Desert, Egypt. Ann. Geol. Surv. Egypt 15, 1–30.

El Aref, M.M., ElSharkawi, M.A., Khalil, M.A., 1999. The geology and genesis of stratabound to stratiform Cretaceous-Eocene iron ore deposits of El Bahariya Region, Western Desert, Egypt. In: Proceeding of International Conference on the Geology of the Arab World (GAW4), pp. 450–475.

El Bassyony, A.A., 2005. Bahariya teetotumensis n. gen. n. sp. from the Middle Eocene of Egypt. Revue de Paléobiologie Genève 24, 319–329.

El Sharkawi, M.A., Higazi, M.M., Khalil, N.A., 1984. Three genetic iron ore dikes of iron ores at El Gedida mine, Western Desert. Egypt. Geol. Soc. Egypt. In: 21st Annual Meeting, Cairo, Egypt (Abstract).

El Shazly, E.M., 1962. Report on the results of drilling in the iron ore deposit of Gebel Ghorabi, Bahariya Oasis, Western Desert. Geol. Surv. Egypt, 25.

Goldberg, E.D., Koide, M., Schmitter, R.A., Smith, R.H., 1963. Rare earth 'distributions in the marine environment. J. Geophys. Res. 68, 4209.

Guichard, F., Church, T.M., Treuil, M., Jaffrezic, H., 1979. Rare earths in barites: distribution and effects on aqueous partitioning. Geochim. Cosmochim. Acta 43, 983–997.

Gültekin, A.H., Orgun, Y., Suner, F., 2003. Geology, mineralogy and fluid inclusion data for Kizilcaoren fluorite-barite-REE deposit, Eskisehir, Turkey. J. Asian Earth Sci. 21, 365–376.

Hanor, J.S., 2000. Barite-celestine geochemistry and environments of formation. Rev. Mineral. Geochem. 40, 193–275.

Haskin, L.A., Freyf., F.A., Schmitter, A.Smithr, H., 1968. Meteoritic, solar and terrestrial rare earth distributions. In: Physics and Chemistry of the Earth. Pergamon Press.

Hein, J.R., Zierenberg, R.A., Maynard, J.B., Hannington, M.D., 2007. Barite-forming environments along a rifted continental margin, Southern California Borderland. Deep-Sea Res. II 54, 1327–1349.

Hofmann, R., Baumann, A., 1984. Preliminary report on the Sr isotopic composition of hydrothermal vein barites in the Federal Republic of Germany. Mineral. Deposit. 19, 166–169.

Hogdahl, T., Melsom, S., Bowenv, T., 1968. Neutron activation analysis of lanthanide elements in sea water. In: Advances in Chemistry, Series No. 73, Am. Chem. Sot., p. 308 (Chapter 19).

Jiang, Y., Elswick, E.R., Mastalerz, M., 2008. Progression in sulfur isotopic compositions from coal to fly ash: examples from single-source combustion in Indiana. Int. J. Coal Geol. 73, 273–284.

Kontak, D.J., Kyser, K., Gize, A., Marshall, D., 2006. Structurally controlled vein barite mineralization in the Maritimes basin of eastern Canada: geological setting, stable isotopes, and fluid inclusions. Econ. Geol. 101, 407–430.

Luders, V., Pracejus, B., Halbach, P., 2001. Fluid inclusion and sulfur isotope studies in probable modern analogue Kuroko-type ores from the JADE hydrothermal field (Central Okinawa Trough, Japan). Chem. Geol. 173, 45–58.

Marchev, P., Moritz, R., 2006. Isotope composition of Sr and Pb in the Central Rhodopean ore fields: inferences for the genesis of the base-metal deposits. Geol. Balcanica 35, 49–61.

Marchev, P., Downes, H., Thirlwall, M.F., Moritz, R., 2002. Small-scale variations of $^{87}Sr/^{86}Sr$ isotope composition of barite in the Madjarovo low-sulphidation epithermal system, SE Bulgaria: implications for sources of Sr, fluid fluxes and pathways of ore forming fluids. Miner. Deposita 37, 669–677.

Matter, A., Peters, T., Ramseyer, K., 1987. $^{87}Sr/^{86}Sr$-Verhältnisse und Sr-Gehalte von Tiefengrundwässern. Mineralien sowie Gesteinen aus dem Kristallin und der Trias der Eclogae Geologicae Helvetiae 80, 579–592.

McLennan, S.M., 1989. Geochemistry of Archean shale from the Pilbara Super group, Western Australia. Geochim. Cosmochim. Acta 47, 1211–1222.

Meneisy, M.Y., El Kaleubi, B.A., 1975. Isotopic ages of the volcanic rocks of Bahariya Oasis. Ann. Geol. Surv. Egypt 119, 99–122.

Monnin, C., Cividini, D., 2006. The saturation state of the world's ocean with respect to (Ba, Sr)SO_4 solid solution. Geochim. Cosmochim. Acta 70, 3290–3298.

Morsy, M.A., 1987. Geology and radioactivity of late Cretaceous-Tertiary sediments in the Northern Western Desert, Egypt (Ph.D. Thesis), Faculty of Science, Mansoura University, Egypt, 351 p.

Nakhla, F.M., 1961. The iron ore deposits of El-Bahariya Oasis, Egypt. Econ. Geol. 56, 1103–1111.

Nakhla, F.M., Shehata, M.R.N., 1967. Contribution to the mineralogy and geochemistry of some iron ore deposits in Egypt. Miner. Deposita 2, 357–371.

Paytan, A., Kastner, M., Campbell, D., Thiemens, M.H., 1998. Sulfur isotope composition of cenozoic seawater sulfate. Science 282, 1459.

Pfaff, K., Hildebrandt, L.H., Leach, D.L., Jacob, D.E., Markl, G., 2010. Formation of the Mississippi Valley-type Zn-Pb-Ag deposit in the extensional setting of the upper Rhinegraben in the Wiesloch area, SW Germany. Miner. Deposita 45, 647–666.

Said, R., 1990. The Geology of Egypt. Elsevier, New York, 734 pp..

Schwinn, G., Wagner, T., Baatartsogt, B., Markl, G., 2006. Quantification of mixing processes in ore-forming hydrothermal systems by combination of stable isotope and fluid inclusion analyses. Geochim. Cosmochim. Acta 770, 965–982.

Scotney, P.M., Roberts, S., Herrington, R.J., Boyce, A.J., Burgess, R., 2005. The development of volcanic hosted massive sulfide and barite-gold ore bodies on Wetar Island, Indonesia. Miner. Deposita 40, 76–99.

Soliman, S.M., El Badry, O.A., 1980. Petrology and tectonic framework of Cretaceous, Bahariya Oasis, Egypt. J. Geol. Soc. Egypt 27, 1153.

Staude, S., Göb, S., Pfaff, K., Ströbele, F., Premo, W.R., Mark, G., 2011. Deciphering fluid sources of hydrothermal systems: a combined Sr- and S-isotope study on barite (Schwarzwald, SW Germany). Chem. Geol. 286, 1–20.

Torres, M.E., Bohrmann, G., Suess, E., 1996. Authigenic barites and fluxes of barium associated with fluid seeps in the Peru subduction zone. Earth Planet. Sci. Lett. 144, 469–481.

Tosson, S., Saad, N.A., 1974. Genetic studies of El-Bahariya iron ore deposits, Western Desert, Egypt. Neus Jahrbuch fur Mineralogie-Abhandlungen 121, 317–393.

Valenza, K., Moritz, R., Mouttaqi, A., Fontignie, D., Sharp, Z., 2000. Vein and karst barite deposits in the western Jebilet of Morocco: fluid inclusion and isotope (S, O, Sr) evidence for regional fluid mixing related to central Atlantic rifting. Econ. Geol. 95, 587–606.

Veizer, J., 1989. Strontium isotopes in seawater through time. Annu. Rev. Earth Planet. Sci. 17, 141–167.

Wagner, T., Kirnbauer, T., Boyce, A.J., Fallick, A.E., 2005. Barite-pyrite mineralization of the Wiesbaden thermal spring system, Germany: a 500-kyr record of geochemical evolution. Geofluids 5, 124–139.

Williams-Jones, A.E., Samson, I.M., Olivo, G.R., 2000. The genesis of hydrothermal fluorite-REE deposits in the Gallinas Mountains, New Mexico. Econ. Geol. 95, 327–342.